High-spin γ-ray spectroscopy in ^{197}Bi

T. Chapuran*
Department of Physics, State University of New York, Stony Brook, New York 11794
and Department of Physics, University of Pennsylvania, Philadelphia, Pennsylvania 19104

K. Dybdal,† D. B. Fossan, T. Lönnroth,‡ and W. F. Piel, Jr.
Department of Physics, State University of New York, Stony Brook, New York 11794

D. Horn§ and E. K. Warburton
Department of Physics, Brookhaven National Laboratory, Upton, New York 11973
(Received 19 August 1985)

The properties of high-spin states in ^{197}Bi have been studied with the ^{192}Pt(^{10}B,5n)^{197}Bi reaction at ^{10}B energies between 50 and 80 MeV. In-beam measurements of γ-ray excitations, γ-γ-t coincidences, γ-ray angular distributions, and pulsed-beam-γ timing were performed with Ge detectors to determine level energies, decay schemes, γ-ray multipolarities, J^π assignments, and isomeric lifetimes. Yrast levels up to $J=\frac{33}{2}$ were established including four isomers. The nuclear structure properties of ^{197}Bi are compared with systematic trends for the heavier odd-mass Bi isotopes.

I. INTRODUCTION

Nuclear structure studies of the odd-mass Bi isotopes[1-7] under the changing stress of the neutron-proton imbalance provide a sensitive probe into the underlying physics. The high-spin structure of these isotopes has previously been explored out to ^{199}Bi ($N=116$),[1] ten neutrons away from the closed shell at $N=126$. The yrast cascades in these nuclei are understood in terms of one- and three-quasiparticle states involving the odd-proton orbitals coupled to the neutron-hole states in the even-A Pb cores. The particular states observed, and their systematic behavior as a function of neutron number, are consistent with a shell-model weak-coupling interpretation. Electromagnetic transition strengths (determined from measurements of isomeric lifetimes) imply no more than a small enhancement of collective effects in the lightest isotopes studied thus far.

In this paper, we extend our investigations of the quasiparticle and collective properties of the odd Bi isotopes to a greater neutron-proton imbalance with our results for ^{197}Bi ($N=114$). High-spin states have been populated via the (^{10}B,5n) reaction; since no prior information on excited states in ^{197}Bi was available, a clean identification of the reaction channel was required. The interpretation of the experimental results is aided by knowledge of the ^{196}Pb core structure.[8] Quasiparticle cluster-interaction calculations (similar to those discussed previously[1]) are compared with the observed level scheme of ^{197}Bi. An examination of the electromagnetic transition strengths is also made to probe possible changes in the nuclear structure as a function of neutron deficiency. A further extension of these studies into ^{195}Bi ($N=112$) will be presented in a subsequent paper.[9]

II. EXPERIMENTAL PROCEDURE

High-spin states of ^{197}Bi were populated using the ^{192}Pt(^{10}B,5n) reaction with 50–80 MeV ^{10}B beams from the Brookhaven National Laboratory Van de Graaff accelerator. The target, which was 3 mg/cm^2 thick, was enriched to 57% in ^{192}Pt. Competing reactions induced in the 40% ^{194}Pt target component were identifiable from measurements with a pure ^{194}Pt target made during our study of the ^{194}Pt(^{10}B,5n)^{199}Bi reaction.[1] The deexcitation γ rays were detected with Ge(Li) detectors having energy resolutions of 2.0–2.2 keV and efficiencies of 10–20% (relative to a 7.6 cm$\times$7.6 cm NaI detector) at 1.33 MeV. A 7 mm thick planar intrinsic Ge detector was also used in the lifetime measurements for increased sensitivity to low energy γ rays.

Excitation functions were measured in 5 MeV steps for $E_{lab}=50$–80 MeV. Activity spectra were also obtained over two two-minute periods following each in-beam measurement, to aid in the identification of the reaction products. Gamma-gamma-time coincidence measurements were performed with Ge(Li) detectors at $+90°$ and $-112°$ at a beam energy of 72 MeV. The γ-ray angular distributions were measured at seven angles between 75° and 160° with respect to the beam direction using a detector 18 cm from the target, while a second detector at $-90°$ served as a monitor. The function $W(\theta)=I_\gamma(1+A_2P_2+A_4P_4)$ was fitted to these data to obtain the relative γ-ray intensity I_γ and the Legendre polynomial coefficients A_2 and A_4. Mixing ratios were extracted for several $M1/E2$ transitions using alignments obtained from pure-multipole transitions following these reactions. Lifetimes of isomeric states were measured using 72 MeV ^{10}B beam pulses having a width of about 10 nsec and a repetition period of 2 μsec. A coaxial Ge(Li) detector and planar intrinsic Ge

(at $\pm 90°$) were used for these measurements. Additional lifetime information was extracted from the $\gamma-\gamma-t$ coincidence data, which were taken with a time range of 500 nsec.

III. EXPERIMENTAL RESULTS

The identification of ^{197}Bi is based on the in-beam and activity γ excitation functions and on the observation of γ-x-ray coincidences. The excitation functions show contributions from ^{10}B reactions on both of the dominant target components, ^{192}Pt and ^{194}Pt. Based on Q values, the evaporation reactions on ^{192}Pt are expected to peak at bombarding energies ~ 3 MeV higher than the corresponding reactions on ^{194}Pt. The lower portion of Fig. 1 shows the yields of the ground-state transitions[8] in ^{198}Pb and ^{196}Pb extracted from the out-of-beam measurements. These γ rays can arise solely from the decays of 11.8 min ^{198}Bi and 4.5 min ^{196}Bi, respectively. The two peaks in the ^{198}Pb excitation function result from production of ^{198}Bi in the ^{192}Pt(^{10}B,4n) and ^{194}Pt(^{10}B,6n) reactions, while the ^{196}Pb comes from decay of ^{196}Bi produced in the ^{192}Pt(^{10}B,6n) reaction. These curves indicate clearly that ^{198}Bi and ^{196}Bi are being produced and that the cross section for ^{197}Bi should peak slightly above 70 MeV. The in-beam excitation functions (see top portion of Fig. 1) show the ^{194}Pt(^{10}B,5n)^{199}Bi reaction peaking roughly halfway between the 4n and 6n peaks of the ^{198}Bi yield. A number of intense γ rays, including the 1009 keV transition, were found to have similar excitation functions, but peaking a few MeV higher than ^{199}Bi. These γ rays were not observed in similar measurements with an enriched ^{194}Pt target, and therefore arise from the ^{192}Pt in the target. The coincidence measurements (see below) indicate that they are part of a cascade which is itself in coincidence with the bismuth K x rays, and which therefore is produced by xn evaporation. The excitation function then shows that this cascade must be assigned to the ^{192}Pt(^{10}B,5n)^{197}Bi reaction. Also shown in Fig. 1 are two of the strongest charged-particle evaporation channels identified, ^{194}Pt(^{10}B,p4n)^{199}Pb and ^{194}Pt(^{10}B,α3n)^{195}Tl. While the pxn and αxn cross sections are significant, the pure neutron-evaporation channels remain the strongest. On the basis of the excitation functions, 72 MeV was chosen as the optimum bombarding energy for all other measurements of ^{197}Bi.

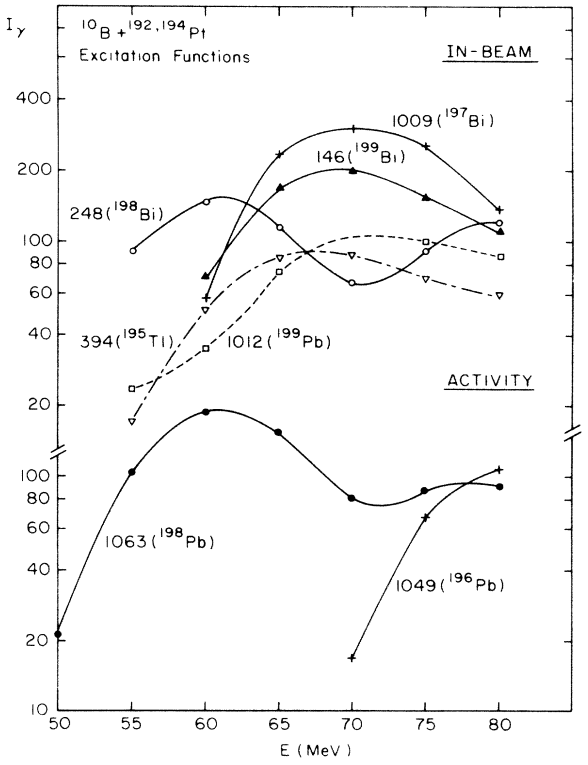

FIG. 1. Yields of γ rays produced by reactions of ^{10}B beams with a target of 57% ^{192}Pt and 40% ^{194}Pt as a function of bombarding energy, measured in beam and out of beam. The yields, which are plotted in arbitrary units, have been corrected for detector efficiency but not for differing branching ratios or half-lives. The γ-ray energies are in keV.

An open-gated coincidence spectrum obtained in the 90° detector is shown in the top portion of Fig. 2. Also shown in Fig. 2 are two Compton-subtracted spectra gated on the $\frac{17}{2}^+ \rightarrow \frac{9}{2}^-$ (g.s.) cascade (a total of six transitions) identified in ^{197}Bi. The middle spectrum shows γ rays arriving within ± 50 nsec of the gating transitions. The lower spectrum excludes the prompt coincidences, and shows γ rays which preceded the gating transitions by at least 20 nsec, indicating the presence of at least one isomer. Three gated spectra were obtained for each of the γ rays studied, with prompt, prior-prompt and post-prompt conditions set on the timing spectrum. These data helped to locate four isomers in ^{197}Bi, and placed constraints on the ordering of transitions in the cascade. Note also the clear presence in the gated spectra of Bi K x rays which arise in part from internally converted transitions depopulating isomeric states. Lifetime information and prompt and delayed intensities were extracted from the coincidence data and from pulsed-beam-γ timing measurements. Examples of pulsed-beam timing spectra and lifetime fits are shown in Figs. 3 and 4. Transition energies, relative γ-ray intensities, and angular distribution coefficients for γ rays assigned to ^{197}Bi are collected in Table I. The experimental lifetime results extracted for ^{197}Bi are summarized in Table II. Spin and parity assignments are based on the angular distributions, the observed lifetimes, and conversion-coefficient limits extracted from the relative γ-ray intensities. The level scheme constructed for ^{197}Bi on the basis of these experimental results is shown in Fig. 5.

The ground state of ^{197}Bi almost certainly has spin and parity $J^\pi = \frac{9}{2}^-$, based on the systematics of the even-even Pb cores[8] and of the single-proton states in the heavier odd Bi isotopes.[1-3] The 1001 and 1196 keV ground state transitions have angular distributions characteristic of stretched quadrupoles, with attenuation coefficients $\alpha_2 = A_2(\text{expt})/A_2(\text{theor})$ of 0.43 ± 0.07 and 0.48 ± 0.05, respectively. This defines two spin $\frac{13}{2}$ states connected by the 196 keV transition, whose angular distribution is consistent with a pure $\Delta J = 0$ dipole. The observed γ-ray intensities rule out an $M1$ assignment for this transition

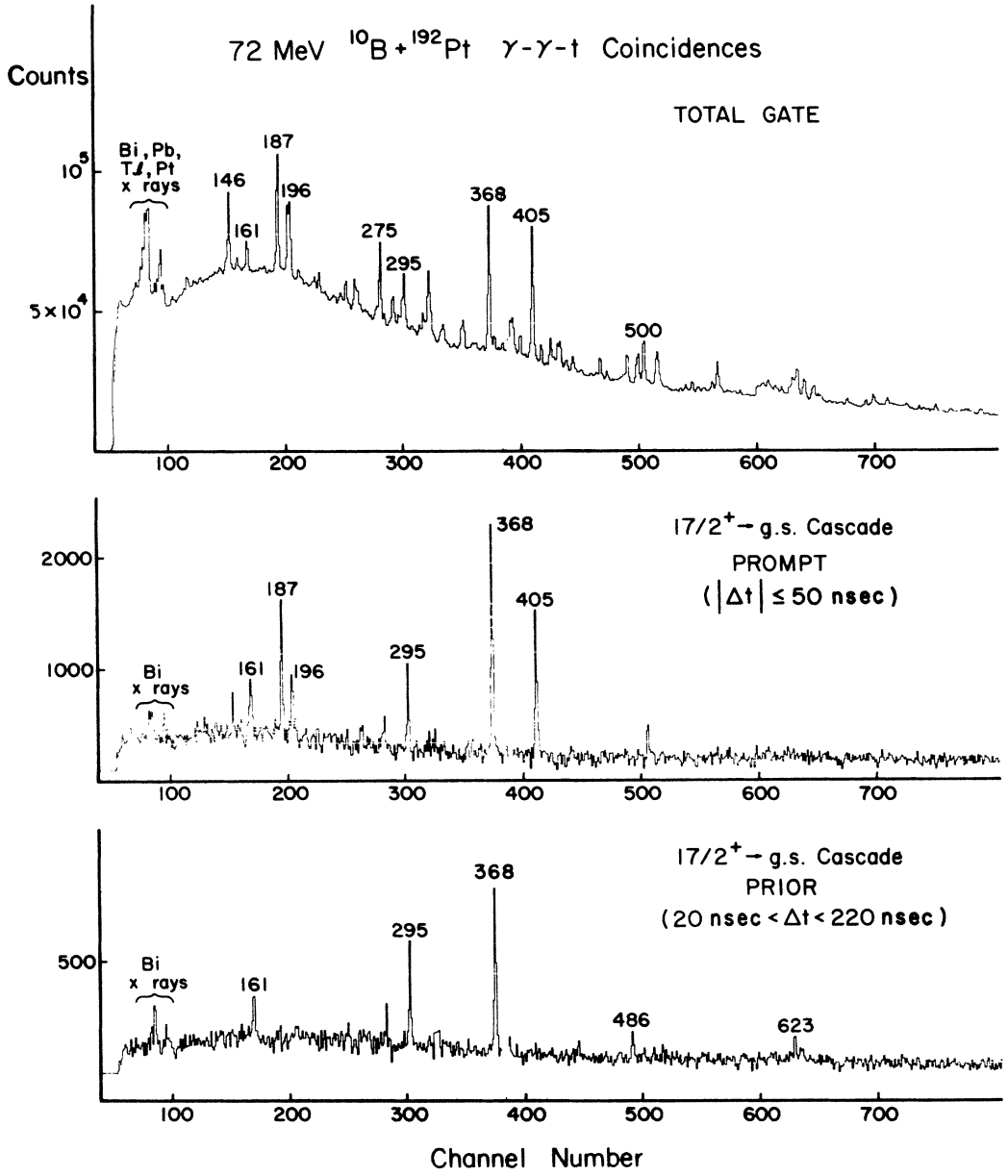

FIG. 2. γ-ray coincidence spectra obtained with the 90° detector from bombardment of an enriched ^{192}Pt target with a 72 MeV ^{10}B beam. A portion of the open-gated coincidence spectrum is shown in the top figure. Each of the two lower curves is a sum of six spectra gated on transitions in the $\frac{17}{2}^+ \rightarrow \frac{9}{2}^-$ (g.s.) cascade in ^{197}Bi. Compton backgrounds have been subtracted using gates set on appropriate regions above or below the full energy peaks. The middle spectrum was projected with a wide gate on the prompt peak in the timing spectrum ($|\Delta t| \leq 50$ nsec between the times of arrival). The lower spectrum shows only γ rays preceding the gated transitions (20 nsec $< \Delta t <$ 220 nsec). Gamma ray energies are labeled in units of keV.

(since the $M1$ total conversion coefficient $\alpha_{M1} = 1.6$), thus indicating opposite parities for the two $\frac{13}{2}$ states. The large negative A_2 value for the 1009 keV transition indicates a $\Delta J = 1$ $M1/E2$ transition with a negative mixing ratio $\delta = -0.38 \pm 0.14$. The 187 keV transition is then a $\frac{13}{2} \rightarrow \frac{11}{2}^-$ dipole, and as the γ-ray intensities again rule out an $M1$ assignment, the parities of the two $\frac{13}{2}$ states are determined as shown in Fig. 5.

The $\frac{13}{2}^+$ state at 1196 keV is fed through the 405 and 368 keV quadrupole transitions, which are identified as electric in character since the $M2$ total conversion coefficients ($\alpha_{M2} \approx 0.7$—0.9) would result in total intensities significantly greater than the sum of the ground state transitions. Above the 1969 keV $\frac{21}{2}^+$ level, the cascade is again fragmented, with the main feeding coming through a cascade of three dipole transitions of 295, 486, and 439 keV. However, the 295 keV γ ray is known from the coincidence data to precede the 386 keV transition in time, corresponding to an isomer of half-life $t_{1/2} \approx 60$ nsec. Since the 386 keV transition shows a clear prompt peak in the pulsed beam data, there must be another transition depopulating the isomer. This transition could not be

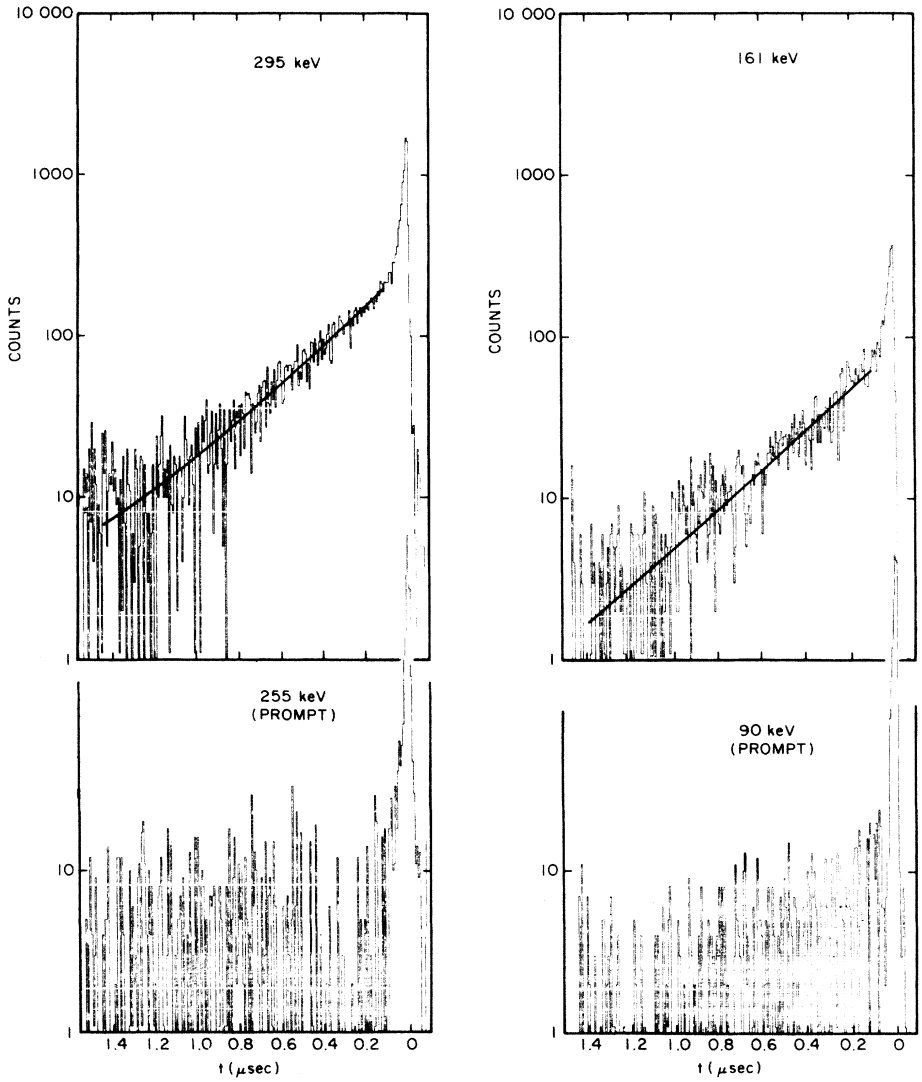

FIG. 3. Pulsed-beam timing spectra for the 295- and 161-keV transitions in ^{197}Bi. The single-lifetime fits yield half-lives of 263±13 nsec and 240±18 nsec, respectively. The 161 keV data were taken with the planar detector. Note that both transitions have clear prompt peaks. The timing spectra for prompt transitions at nearby energies are shown for comparison.

identified in the individual coincidence gates, as would be expected for a low energy γ ray subject to significant conversion and strong absorption. The pulsed beam γ-timing measurements with a planar Ge detector produced a candidate for this transition, at 97 keV, which shows the expected lifetimes in its decay (see the discussion below). However, the situation is further complicated by a contaminant in the 97 keV photopeak window from unidentified activity, as can be seen from the flat, time-independent background in Fig. 4. An intensity of $I_\gamma = 12 \pm 5$ was estimated for the transition of interest from the pulsed-beam and angular distribution data. The large uncertainties associated with the A_2 and A_4 coefficients (see Table I) reflect the difficulty of extracting peak areas; this is partly due to the high Compton background of the Ge(Li) detector at this energy. Nevertheless, the A_2 coefficient is clearly positive while the γ-ray intensity rules out an $M2$ assignment, but is consistent within the errors with an $E2$ assignment ($\alpha_{M2}=98$, $\alpha_{E2}=7.8$). This identifies the isomer as a $\frac{25}{2}^+$ state. While the identification of the 97 keV transition with the isomeric decay must be considered tentative, the spin assignment is independently favored strongly by the systematics of the odd-mass Bi isotopes.

Above the $\frac{25}{2}^+$ state, the 295 keV transition is preceded in time by the 486-439 keV cascade. The upper transitions, which are prompt, feed the 295 keV transition through an isomer with $t_{1/2}=263\pm13$ nsec (see Fig. 3). The prompt peak in the 295 keV pulsed beam spectrum suggests that the isomer lies just above the 2360 keV level and is depopulated by an unobserved transition. Only a low energy ($E_\gamma \lesssim 100$ keV) $E1$ or $E2$ transition would be consistent with both the measured lifetime and the absence of a peak in the coincidence data. An $E1$ transition ($\frac{29}{2}^- \rightarrow \frac{27}{2}^+$) would be expected from the systematics of the $\frac{29}{2}^-$ isomers observed in the heavier odd Bi isotopes

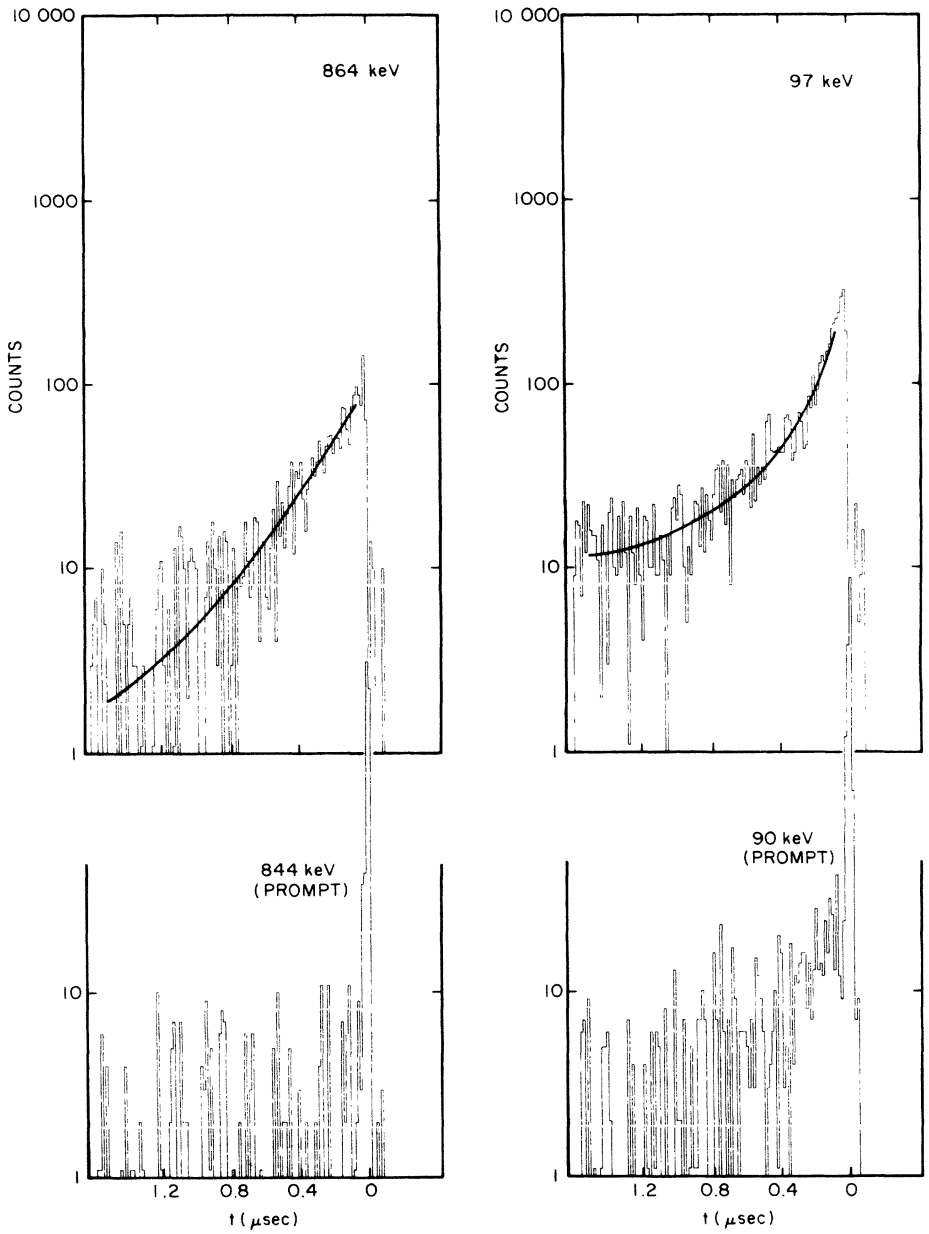

FIG. 4. Pulsed-beam timing spectra for the 864- and 97-keV transitions in ^{197}Bi. A single-lifetime fit shown for the 864 keV transition yields a half-life of 209±30 nsec. The 97 keV transition (observed with the planar detector) is fed through three isomers; see the text for discussion.

(see Sec. IV). A search for low energy delayed γ rays with the planar Ge detector produced no candidates for this transition, suggesting that $E_\gamma \lesssim 40$ keV. Above the isomer, the large negative A_2 coefficients for the 486 and 439 keV transitions indicate $\Delta J=1$ $M1/E2$ transitions with negative mixing ratios ($\delta=-0.33\pm0.18$ and -0.37 ± 0.21, respectively).

Finally, the most probable spin and parity of the 2929 keV isomeric level is suggested to be $(\frac{31}{2}^-)$. The pulsed beam timing spectrum for the 864 keV transition (see Fig. 4) shows that it depopulates an isomer of half-life $t_{1/2}=209\pm30$ nsec. This half-life for such a high energy transition, when combined with the positive A_2 coefficient, indicates a high multipolarity, namely $M2$ or $E3$. An $M2$ assignment would be unlikely since a considerably shorter half-life would be expected based on known $B(M2)$ values in this region [e.g., $t_{1/2}=8$ nsec would be predicted using the measured $B(M2)$ for the $\frac{13}{2}^+ \rightarrow \frac{9}{2}^-$ transition[10] in ^{201}At]. On the other hand, an $E3$ assignment gives a transition probability which lies within the expected range of values. The nature of the two closely spaced $(\frac{31}{2}^-)$ states at 2846 + Δ and 2929 keV will be discussed in Sec. IV.

Half-lives of five isomeric states in ^{197}Bi have been obtained from the pulsed beam and coincidence measurements. One isomer, which could not be placed in the level scheme, was observed through its feeding of the 2129 keV $(\frac{23}{2}^-)$ state, as seen in the pulsed beam spectrum of the

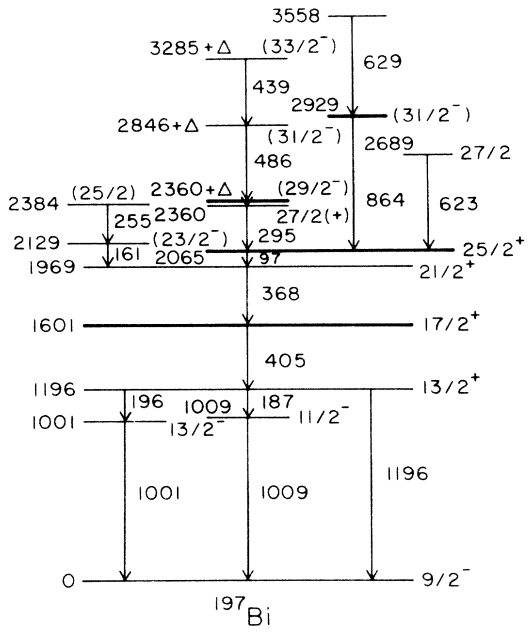

FIG. 5. Energy level scheme for ^{197}Bi determined in the present work. Energies are given in keV. Tentative assignments are enclosed in parentheses. The four isomeric levels are indicated by thick lines.

161 keV transition shown in Fig. 3. The half-life determined from the fit is $t_{1/2}=240\pm18$ nsec. The half-lives of two other isomers were determined from single lifetime fits to the 295 and 864 keV transitions, as shown in Figs. 3 and 4 and previously discussed. The 97 keV $\frac{25}{2}^+ \rightarrow \frac{21}{2}^+$ transition is fed through these latter two isomers ($t_{1/2}=263\pm13$ nsec and 209 ± 30 nsec, respectively), while depopulating a third isomer. A value for the $\frac{25}{2}^+$ half-life of $t_{1/2}=60\pm22$ nsec was determined from fits to the coincidence timing spectrum taken between the 368 and 295 keV transitions, which is influenced only by that one lifetime. Then the 97 keV pulsed beam data were fit using the known lifetimes, feeding patterns, and intensities, and varying the prompt sidefeeding and a background term. The resulting fit (see Fig. 4) shows the consistency of the pulsed beam data with the proposed level scheme. Due to the uncertainties in all of the input parameters and to the complexity of the decay scheme, the coincidence data constrain the lifetime more stringently than the pulsed beam data, and therefore we adopt the half-life quoted above.

The lowest isomer in the decay scheme is the $\frac{17}{2}^+$ state at 1601 keV, which is fed by all four of the other isomers. The pulsed beam γ-timing spectrum for the 405 keV transition [see Fig. 6(a)] is correspondingly complicated, but an accurate half-life can be obtained from the coincidence timing data. Figure 6(b) shows the timing spectrum gated on the 368 and 405 keV transitions, which clearly shows only a single lifetime, the fit corresponding to $t_{1/2}=16.8\pm1.9$ nsec. When combined with similar fits to the 368—1001 keV and 368—1009 keV timing spectra, a final result of $t_{1/2}=16.2\pm1.7$ nsec is obtained. Shown in Fig. 6(a) is a fit to the pulsed-beam data using this value and the previously determined lifetimes and feeding patterns and intensities, varying only the prompt side feeding of the lowest two isomeric levels. A good fit is obtained for reasonable values of the parameters, showing the consistency of the pulsed beam and the coincidence data. Due to the uncertainties in the input parameters and the complexity of the five-lifetime formula, the pulsed beam data only restrict the $\frac{17}{2}^+$ half-life to a range of $t_{1/2}=10$—40 nsec, and therefore the more accurate value obtained from the cleaner coincidence data has been adopted as the final result.

IV. DISCUSSION

The discussion below is divided into two subsections. Subsection A deals with the identification of the quasiparticle configurations, the extension of the odd-mass Bi excitation-energy systematics, and a compairson of the observed level energies with the results of quasiparticle cluster-interaction calculations. Subsection B includes our results for electromagnetic transition strengths in ^{197}Bi, and a discussion of the systematics of these strengths throughout the neutron-deficient odd-mass Bi isotopes.

A. Excitation energies and configuration assignments

The experimental level scheme of ^{197}Bi has been presented in Fig. 5. The interpretation of the yrast states in the heavier odd-mass Bi isotopes in terms of quasiparticle excitations has been discussed in detail previously.[1] Due to the large number of valence particles involved (1 proton particle and 12 neutron holes in the case of ^{197}Bi), a shell-model description relative to a ^{208}Pb core is not tractable. However, the excited states in the odd Bi isotopes can be described as arising from weak coupling of the valence proton with the predominantly two-quasiparticle (neutron-hole) states in the even-A Pb cores.[1-7] Under this assumption, the states are of the form

$$|J,^{A+1}\mathrm{Bi}\rangle = |\nu I,^{A}\mathrm{Pb}\rangle \otimes |j_p\rangle ,$$

where J is the spin of the state in the odd $^{A+1}$Bi nucleus, I is the spin of the core state in the even ^{A}Pb nucleus, and j_p refers to the valence proton orbital. The excitation energies of the corresponding states in the $^{A+1}$Bi and ^{A}Pb nuclei can then be related by

$$E(J,^{A+1}\mathrm{Bi}) = E(I,^{A}\mathrm{Pb}) + E(j_p) - \Delta(I \otimes j_p; J) ,$$

in which the last term is called the cluster interaction energy.[1] For states involving the lowest energy proton orbital $\pi h_{9/2}$, for which we take $E(j_p)=0$, the cluster interaction energy is given by

$$\Delta(I \otimes \pi h_{9/2}; J) = E(I,^{A}\mathrm{Pb}) - E(J,^{A+1}\mathrm{Bi}) .$$

To the extent that the neutron-hole configurations in the core excitations remain constant from one Pb isotope to the next, the interaction energies should also remain constant. In this case, the systematics of the levels in the odd Bi isotopes would just follow the behavior of the core states. In some cases, the core configurations are expected to change in moving towards the lighter isotopes, as the Fermi level drops progressively further into the neutron

TABLE I. Properties of γ rays assigned to transitions in ^{197}Bi from the ^{192}Pt(^{10}B,5n)^{197}Bi reaction.

E_γ (keV)[a]	I_γ (%)[b]	A_2	A_4	$J_i^\pi \rightarrow J_f^\pi$
96.9	12[c]	0.36(11)[d]	−0.13(16)[d]	$\frac{25}{2}^+ \rightarrow \frac{21}{2}^+$
160.7	16	−0.08(2)	−0.02(3)	$(\frac{23}{2}^-) \rightarrow \frac{21}{2}^+$
187.0	≈40[e]	−0.04(1)[f]	−0.02(2)[f]	$\frac{13}{2}^+ \rightarrow \frac{11}{2}^-$
195.6	33	0.19(2)	0.00(2)	$\frac{13}{2}^+ \rightarrow \frac{13}{2}^-$
255.2	≤9[c]	−0.19(6)	−0.01(1)	$(\frac{25}{2}) \rightarrow (\frac{23}{2}^-)$
294.9	29	−0.12(1)	−0.01(2)	$\frac{27}{2}^{(+)} \rightarrow \frac{25}{2}^+$
367.6	85[e]	0.10(3)[g]	0.00(4)[g]	$\frac{21}{2}^+ \rightarrow \frac{17}{2}^+$
404.7	100	0.14(1)	−0.02(1)	$\frac{17}{2}^+ \rightarrow \frac{13}{2}^+$
438.9	8	−0.38(3)	0.02(5)	$(\frac{33}{2}^-) \rightarrow (\frac{31}{2}^-)$
485.6	17	−0.38(2)	−0.04(2)	$(\frac{31}{2}^-) \rightarrow (\frac{29}{2}^-)$
623.2	6	−0.24(5)	−0.02(9)	$\frac{27}{2} \rightarrow \frac{25}{2}^+$
628.8[h]				$\rightarrow (\frac{31}{2}^-)$
864.0	13	0.08(3)	−0.03(4)	$(\frac{31}{2}^-) \rightarrow \frac{25}{2}^+$
1000.8	≥44[e]	0.19(3)[i]	−0.07(5)[i]	$\frac{13}{2}^- \rightarrow \frac{9}{2}^-$
1009.2	59	−0.37(1)	0.03(2)	$\frac{11}{2}^- \rightarrow \frac{9}{2}^-$
1196.2	21	0.21(2)	0.04(3)	$\frac{13}{2}^+ \rightarrow \frac{9}{2}^-$

[a]Energies obtained from angular distribution and coincidence measurements; accurate to ±0.2 keV except where noted.

[b]γ-ray intensities normalized to the 404.7 keV yield, accurate to ±10% for $E_\gamma \geq 200$ keV, ±20% for $E_\gamma < 200$ keV except where noted.

[c]Estimated from pulsed beam data. Contaminated by an activity line in singles. See the text for discussion.

[d]The errors have been increased by a factor of 2.7 to reduce χ^2/N to 1.

[e]I_γ estimated from coincidence data.

[f]Includes contribution from an unidentified contaminant with $I_\gamma \approx 20$.

[g]Includes contribution from unresolved 367 keV (^{199}Tl) activity with $I_\gamma \approx 40$.

[h]Energy accurate to ±0.5 keV; line unresolved from the neighboring contaminants in singles.

[i]Includes a small contribution from the 1002 keV (^{199}Bi) stretched quadrupole.

shell. Then the cluster interaction energies should vary smoothly for slowly changing configurations. Furthermore, the signs of the variations should be understandable on the basis of the known proton-neutron hole interaction energies for the particular orbitals involved.

In a previous paper,[1] cluster interaction energies extracted from ^{203,205}Bi were used along with the yrast spectra of ^{198,200}Pb to calculate the expected locations of the three-quasiparticle states in ^{199,201}Bi. Good agreement was obtained with the empirically determined level schemes. To extend these calculations to ^{197}Bi, the cluster interaction energies and their variations have been extracted from the four heavier odd-A isotopes $^{199-205}$Bi. (^{207}Bi was generally not used due to the strong influence of the $p_{1/2}$ neutron-hole orbit.) The cluster interaction energies are listed in Table III. The values used for the ^{197}Bi calculation were obtained either from the mean of values extracted from the heavier isotopes, or from a linear extrapolation when systematic variations were observed. In some cases the behavior of the interaction energies versus mass is not well defined, and there is some arbitrariness in the extrapolations. In most cases, however, the uncertainties in extrapolating to values for ^{197}Bi are believed to be less than ±50 keV.

The cluster interaction energies from Table III were used together with the level scheme[8] of ^{196}Pb to calculate the excitation energies of three-quasiparticle states in ^{197}Bi. The calculated values are compared with experiment in Fig. 7. Only calculated states predicted to lie near the yrast line are shown; in almost all cases these involve coupling of the valence proton in the $h_{9/2}$ orbital to the core excitations. The spins and parities and the ordering and spacings of these levels are similar to those observed experimentally. Identifying the calculated three-quasiparticle excitations with the empirical states, a mean deviation (rms deviation) of −45 keV (83 keV) from the experimental level energies is found. These values are comparable with the results obtained for ^{199,201}Bi. Thus, as expected, the accuracy of the method is not strongly dependent on the number of valence nucleons, as will be further shown in a subsequent report[9] on ^{195}Bi. The systematics of the excitation energies for $^{197-207}$Bi are shown in Fig. 8, where the states are identified according to the quasiparticle interpretation. The new states observed in

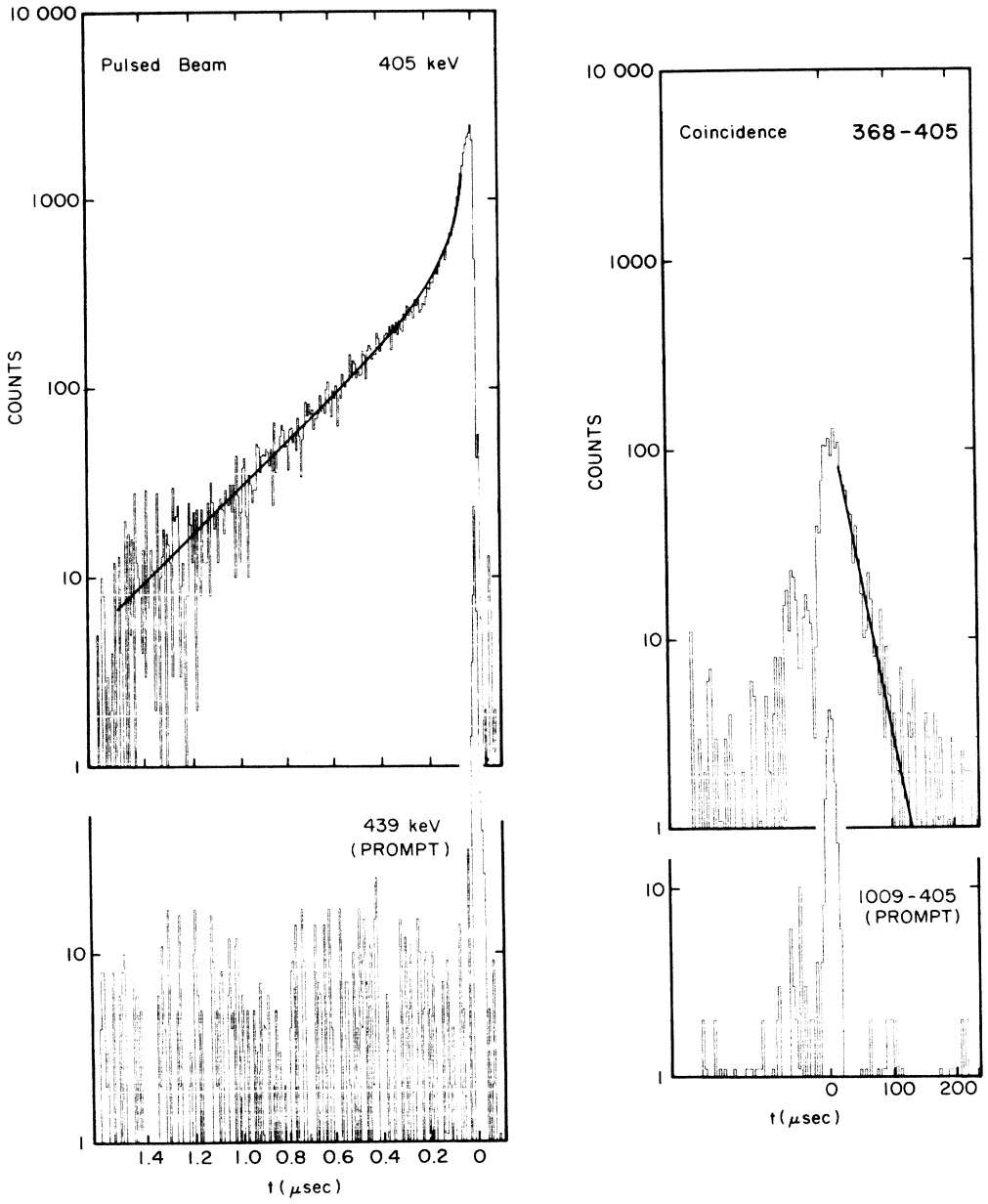

FIG. 6. (a) Pulsed-beam timing spectrum for the 405 keV transition in ^{197}Bi. (b) γ-γ-timing spectrum gated on the 368 and 405 keV transitions in ^{197}Bi. See the text for discussion.

TABLE II. Lifetime results for ^{197}Bi obtained both from γ-γ-t coincidence data (500 nsec time range) and from pulsed-beam-γ timing data (2 μsec repetition period).

E (keV)	J^{π}	$t_{1/2}$ (nsec)
1601	$\frac{17}{2}^+$	16.2± 1.7
2065	$\frac{25}{2}^+$	60 ±22
2360+Δ	$(\frac{29}{2}^-)$	263 ±13
2929	$(\frac{31}{2}^-)$	209 ±30

^{197}Bi generally fit well into the systematics. The excitation energies follow the energies of the core excitations in most cases, and obey the semiempirical J_{max}-1 rule[11] (with the exception of the $h_{9/2}\otimes 2^+$ multiplet).

A striking feature of the systematics is the very rapid decrease in energy of the $\frac{13}{2}^+$ state. This state, which involves the odd proton orbital $\pi i_{13/2}$ coupled to the 0^+ ground state of the Pb core, drops lower in energy than expected from the calculation in ^{197}Bi. This is probably due to an accelerated (rather than linear) increase of the population of neutron holes in the $\nu i_{13/2}$ orbital. The

TABLE III. Cluster-interaction energies of $|J,^{A+1}\mathrm{Bi}\rangle = |\nu I,^{A}\mathrm{Pb}\rangle \otimes |j_p\rangle$ quasiparticle states in odd Bi isotopes.

			$\Delta(I\otimes j_p;J)$ keV					
νI^π	j_p	J^π	^{207}Bi	^{205}Bi	^{203}Bi	^{201}Bi	^{199}Bi	^{197}Bi[a]
0^+	$i_{13/2}$	$\frac{13}{2}^+$	+1	+17	+48	+107	+213	+250
2^+	$h_{9/2}$	$\frac{11}{2}^-$	+133	+103	+78	+63	+30	+10 ext
		$\frac{13}{2}^-$	−129	+18	+28	+60	+62	+80 ext
4^+	$h_{9/2}$	$\frac{15}{2}^-$	+38	+105	+135	+110		+120 *m* 3
		$\frac{17}{2}^-$		−71	−116	+15	+124	+70 *m* 2
5^-	$h_{9/2}$	$\frac{17}{2}^+$		+217	+136	+157	+175	+170 *m*
7^-	$h_{9/2}$	$\frac{21}{2}^+$	+98	+200	+217	+222	+245	+260 ext
9^-	$h_{9/2}$	$\frac{25}{2}^+$	+57	+80	+137	≈ +240	+188	+230 ext
		$\frac{27}{2}^+$	−842	−561	−552	≈ −350	−305	−100 ext
12^+	$h_{9/2}$	$\frac{29}{2}^-$	+139	+169	+214	≈ +200	+158	+180 *m*
		$\frac{31}{2}^-$	−533	−347	−284	≈ −290	−337	−310 *m* 4
		$\frac{33}{2}^-$		−471	−580	≈ −575	−720	−800 ext
14^+	$h_{9/2}$	$\frac{35}{2}^-$		+3	−370	≈ −110	(−260)	−250 *m* 3
16^+	$h_{9/2}$	$\frac{37}{2}^-$		−159		+280	(+102)	(∼+100)

[a]Values used for the ^{197}Bi calculation. Obtained from heavier isotopes as follows: *m* is the mean of all values; *mN* is the mean of *N* adjacent isotopes; ext is the linear extrapolation.

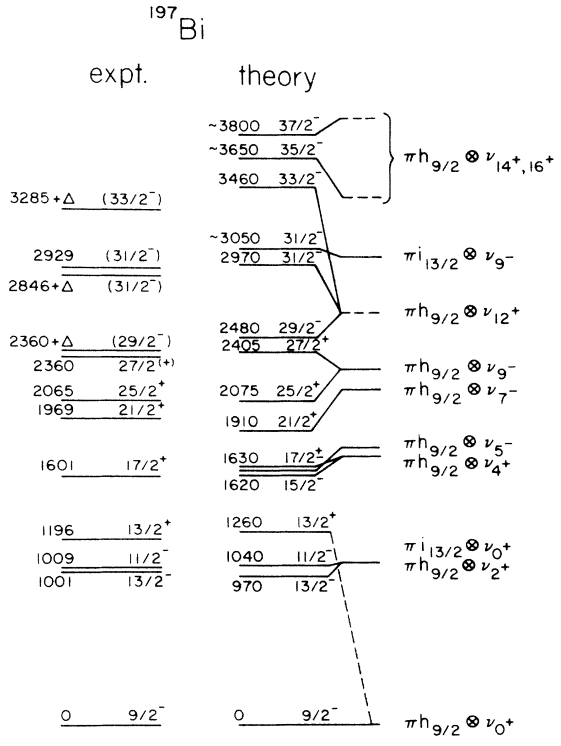

FIG. 7. Comparison of the calculated excitation energies with the experimental values for ^{197}Bi (see the text for discussion).

mean $\pi i_{13/2}\nu i_{13/2}^{-1}$ interaction is less repulsive than for the other $\pi i_{13/2}\nu^{-1}$ pairs, while the mean $\pi h_{9/2}\nu i_{13/2}^{-1}$ interaction is the most repulsive of the $\pi h_{9/2}\nu^{-1}$ pairs. This explains the rapid drop of the $\frac{13}{2}^+$ energy relative to the $\frac{9}{2}^-$ state. The systematics imply that in ^{195}Bi the $\frac{13}{2}^+$ state will drop below the $\frac{11}{2}^-$ and $\frac{13}{2}^-$ states from the $h_{9/2}\otimes 2^+$ configuration and become yrast; this has in fact recently been observed[9] in ^{195}Bi.

The $\pi i_{13/2}$ orbital is also apparently responsible for a second $\frac{31}{2}^-$ level in ^{197}Bi lying less than 80 keV above the $\frac{31}{2}^-$ ($\pi h_{9/2}\otimes 12^+$) state seen in all the odd Bi isotopes. The new level, which has a half-life of 209 nsec, is suggested to have the configuration

$$|\tfrac{31}{2}{}_2^-\rangle = \alpha\,|\pi i_{13/2}\nu(f_{5/2}^{-1}i_{13/2}^{-1})_{9^-};\tfrac{31}{2}^-\rangle + \sqrt{1-\alpha^2}\,|\pi i_{13/2}\nu(f_{7/2}^{-1}i_{13/2}^{-1})_{9^-,10^-};\tfrac{31}{2}^-\rangle\ .$$

In the heavier isotopes, the 9^- core excitation is believed to arise predominantly from the $\nu f_{5/2}^{-1}\nu i_{13/2}^{-1}$ configuration, as the $\nu f_{7/2}^{-1}$ is a deep-lying hole orbit. However, the excitation energy of $\nu f_{7/2}^{-1}$ relative to $\nu f_{5/2}^{-1}$ decreases rapidly[1] to approximately 1 MeV in ^{196}Pb, and therefore the $\frac{31}{2}^-$ component involving this orbital may well be significant. If only the $\nu f_{5/2}^{-1}$ component were considered, the $J_{\max}-1=\frac{29}{2}^-$ state of that multiplet should come lower in energy, but such a state has not been observed. A comparison of the energy difference between the $\frac{31}{2}{}_2^-$ and

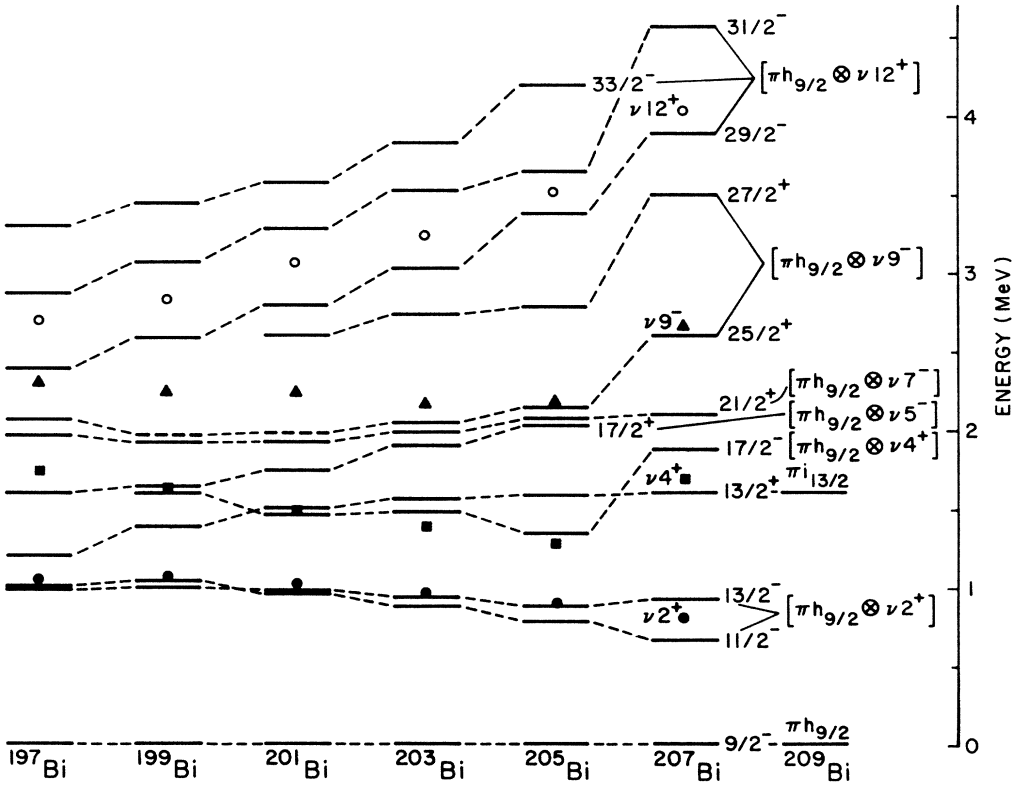

FIG. 8. Comparison of level energies for odd-mass Bi isotopes. Results for ^{197}Bi are from the present work. Results for $^{199-207}$Bi are from Refs. 1–7. States interpreted as having similar configurations are connected with dashed lines. The circles, squares, and triangles represent the energies of the corresponding excitations in the lead cores.

$\frac{25}{2}^+$ states (predominantly $\pi i_{13/2}\otimes 9^-$ and $\pi h_{9/2}\otimes 9^-$, respectively) with that between the $\frac{13}{2}^+$ and $\frac{9}{2}^-$ states ($\pi i_{13/2}\otimes 0^+$ and $\pi h_{9/2}\otimes 0^+$) also requires over 300 keV more attraction for the $\pi i_{13/2}$ proton in the $\frac{31}{2}^-_2$ state. The inclusion of the $\nu(f^{-1}_{7/2}i^{-1}_{13/2})_{9^-,10^-}$ configurations should give additional attraction. First, since this is not a stretched configuration, there are contributions from the intermediate $J_{\max}-1$ parts, which are less repulsive. Second, although the $\pi i_{13/2}\nu f^{-1}_{7/2}$ interaction energies are not known, the high-J states involve a spin-triplet interaction which should give additional attraction relative to that for $\pi i_{13/2}\nu f^{-1}_{5/2}$, which is in a spin-singlet configuration. Finally, it is known[12] that the $\pi i_{13/2}$, $\nu i^{-1}_{13/2}$, and $\nu f^{-1}_{7/2}$ orbitals couple to the collective octupole vibrations in the lead cores. The effective interaction of the octupole phonon with the valence nucleons in small,[13] thus further reducing the repulsion in these configurations. The $\nu f^{-1}_{7/2}$ component in the $\frac{31}{2}^-$ state would thus tend to lower the excitation energy, as is required. The proposed configuration is also consistent with the observed transition rate, as will be discussed below.

B. Electromagnetic transition strengths

Further information about the nuclear structure of excited states in the odd-A Bi isotopes can be extracted from the electromagnetic transition rates determined from isomeric lifetimes and branching ratios. Four isomeric levels were identified in ^{197}Bi. One of these, the $\frac{31}{2}^-_2$ state, has been observed only in ^{197}Bi, while the others correspond to isomers previously observed in the heavier odd-A Bi isotopes. The systematics of these transition strengths are collected, along with selected strengths for the even-A Pb cores, in Table IV.

The two $\frac{31}{2}^-$ states in ^{197}Bi are separated by less than about 80 keV, and show very little mixing. The lower state and the $\frac{29}{2}^-$ state which it feeds are believed to be members of the $\pi h_{9/2}\otimes 12^+$ multiplet observed in the heavier odd-A Bi isotopes. The $\frac{31}{2}^-_2$ state has no observed branch to the $\frac{29}{2}^-$, but rather decays predominantly to the $\frac{25}{2}^+$ ($\pi h_{9/2}\otimes 9^-$) state via an $E2$ transition. The $\frac{31}{2}^-_2$ half-life of 209 nsec corresponds to a reduced transition probability $B(E3)=5.3$ W.u. This is comparable to the mean value of about 3 W.u. found[14] for nine transitions of the type $\pi i_{13/2}\rightarrow\pi h_{9/2}$ in the lead region. These observations along with the excitation energy considerations discussed in Sec. IV A lead to a suggested configuration of $\pi i_{13/2}\otimes 9^-,10^-$, for the second $\frac{31}{2}^-$ state. Decay of this state to the $\frac{29}{2}^-$ level would then be forbidden in first order since the corresponding configurations cannot be connected via one-body operators.

The $\frac{29}{2}^-\rightarrow\frac{27}{2}^+$ transition was unobserved, but a limit of $E_\gamma \lesssim 40$ keV can be set from the experimental data (see Sec. III). Combined with the measured $\frac{29}{2}^-$ half-life of 263 nsec, this leads to the range of strengths listed in

TABLE IV. Systemtaics of $E1$ and $E2$ transition rates in neutron-deficient even-A Pb and odd-A Bi nuclei relative to single-particle units. (Two values are given when two decay branches are known.)

			Transition probability (W.u.) for $A^{core}=$						
$E\lambda$	Nucleus	Transition	196	198	200	202	204	206	Main configuration
$E1$	Pb	$5^- \rightarrow 4^+$	5.0[a]	0.5[a]	2.0[a]				$\nu i_{13/2}^{-1} p_{3/2}^{-1} \rightarrow \nu f_{5/2}^{-1} p_{3/2}^{-1}$
($\times 10^{-6}$)	Bi	$\frac{29}{2}^- \rightarrow \frac{27}{2}^+$	6–14[b,k]	0.004[c]	0.04/0.002[c]	0.6/0.2[d]	0.4[e]		$\pi h_{9/2} \nu i_{13/2}^{-2} \rightarrow \pi h_{9/2} \nu i_{13/2}^{-1} f_{5/2}^{-1}$
	Bi	$\frac{13}{2}^+ \rightarrow \frac{13}{2}^-$	5.4[b,f]	10[c,f]	10[c,f]				$\pi i_{13/2} \nu 0^+ \rightarrow \pi h_{9/2} \nu 2^+$
		$\rightarrow \frac{11}{2}^-$	7.5[b,f]	4.4[c,f]	4.8[c,f]				
$E2$	Pb	$12^+ \rightarrow 10^+$	0.4–0.5[a,g]	0.6–0.8[a,g]	0.6–0.9[a,g,h]			0.3[h]	$\nu i_{13/2}^{-2}(12^+ \rightarrow 10^+)$
	Pb	$9^- \rightarrow 7^-$	1.2[i]		0.3[i]				$\nu f_{5/2}^{-1} i_{13/2}^{-1} \rightarrow \nu p_{3/2}^{-1} i_{13/2}^{-1}$
	Bi	$\frac{25}{2}^+ \rightarrow \frac{21}{2}^+$	1.8[b]	1.2–1.6[c,g]	1.0–1.4[c,g]	0.7[j,d]	0.6[j,d]		$\pi h_{9/2} \nu f_{5/2}^{-1} i_{13/2}^{-1} \rightarrow \pi h_{9/2} \nu p_{3/2}^{-1} i_{13/2}^{-1}$
	Bi	$\frac{17}{2}^+ \rightarrow \frac{13}{2}^+$	0.043[b]	0.015[c]					$\pi h_{9/2} \nu i_{13/2}^{-1} p_{3/2}^{-1} \rightarrow \pi i_{13/2} \nu 0^+$

[a]Reference 8.
[b]Present work.
[c]Reference 1.
[d]Reference 5.
[e]Reference 4.
[f]Estimated values; see the text for discussion.
[g]Extracted assuming E_γ is between the L- and K-electron edges, 17 keV $< E_\gamma <$ 88 keV.
[h]Reference 16.
[i]Reference 15.
[j]Reference 2.
[k]Calculated for 17 keV $< E_\gamma <$ 40 keV.

Table IV for this transition, which is interpreted as $\pi h_{9/2}\otimes 12^+ \rightarrow \pi h_{9/2}\otimes 9^-$. The $\frac{25}{2}^+ \rightarrow \frac{21}{2}^+$ transition is believed to be essentially a $9^- \rightarrow 7^-$ core transition, with the $\pi h_{9/2}$ valence proton acting as a spectator. The measured half-life $t_{1/2}=60\pm 22$ nsec yields a $B(E2)$ of 1.8 W.u. Finally, the $\frac{17}{2}^+$ isomer has a half-life of 16.2 ± 1.7 nsec. The $\frac{17}{2}^+ \rightarrow \frac{13}{2}^+$ $E2$ decay is hindered by a factor of more than 20. A direct transition between the dominant configurations

$$|\pi h_{9/2}\nu 5^-;\tfrac{17}{2}^+\rangle \rightarrow |\pi i_{13/2}\nu 0^+;\tfrac{13}{2}^+\rangle$$

is forbidden. The transition can proceed, however, via an admixture of $|\pi i_{13/2}\nu 2^+;\frac{17}{2}^+\rangle$ in the initial state. The hindrance for the $\frac{17}{2}^+ \rightarrow \frac{13}{2}^+$ transition is roughly a factor of 3 smaller in ^{197}Bi than has been found[1] in ^{199}Bi. This again indicates the increasing importance of configurations involving the $\pi i_{13/2}$ orbital as the neutron number decreases.

The systematics of transition strengths collected in Table IV show a modest but consistent increase in the $E2$ enhancements for the $\frac{25}{2}^+ \rightarrow \frac{21}{2}^+$ transitions in the lighter Bi isotopes. A similar increase is also observed for the underlying $9^- \rightarrow 7^-$ core transitions[15] in going from ^{200}Pb to ^{196}Pb. These enhancements are consistent with small admixtures of the $\nu 2^+$ state assuming reasonable $2^+ \rightarrow 0^+$ $B(E2)$ strengths. In contrast, the $\nu i_{13/2}^{-2}$ $12^+ \rightarrow 10^+$ strengths[8,16] are roughly constant or slowly decreasing, due to quenching related to the increasing $\nu i_{13/2}^{-1}$ population.

Also shown in Table IV are the systematics for several $E1$ transitions in the Bi and Pb isotopes. A typical $E1$ strength in the lead region is of the order of 0.2×10^{-6} W.u. The reduced transition probabilities for the $5^- \rightarrow 4^+$ transitions in the even Pb isotopes are somewhat enhanced relative to this, particularly for the case of ^{196}Pb. A similar effect is seen in the estimates listed for the $\frac{13}{2}^+ \rightarrow \frac{13}{2}^-, \frac{11}{2}^-$ transition rates in the odd Bi isotopes. The lifetimes of the $\frac{13}{2}^+$ states were too short to be directly measured ($t_{1/2} \lesssim 5$ nsec). Instead, estimates of the partial $E1$ lifetimes were extracted in ^{197}Bi using the observed branching ratios and assuming that the $B(M2)$ value for the $\frac{13}{2}^+ \rightarrow \frac{9}{2}^-$ transition is the same as that recently measured[9] for the corresponding $\pi i_{13/2} \rightarrow \pi h_{9/2}$ transition in ^{195}Bi [$B(M2)=2.7\pm 0.2$ μ_N^2 fm^2]. However, the $(\pi i_{13/2}\pi h_{9/2}^2)_{13/2^+} \rightarrow (\pi h_{9/2}^3)_{9/2^-}$ transition in ^{201}At shows a considerably larger strength[10] [$B(M2)=14\pm 1$ μ_N^2 fm^2]; if this $B(M2)$ were used in the calculation, the resulting $B(E1)$ estimates would be more than a factor of 5 larger than those listed in Table IV. In the case of ^{199,201}Bi, not all of the $\frac{13}{2}^+$ decays were sufficiently strong to be clearly observed in the coincidence gates. The transition energies are known, however, and it is possible to extract relative intensities from the singles data. Using these intensities, the estimates listed in Table IV were made, based on the $B(M2)$ value from ^{195}Bi. Again, much larger $E1$ strengths would be obtained if the ^{201}At $B(M2)$ value were used. The $\frac{13}{2}^+ \rightarrow \frac{13}{2}^-, \frac{11}{2}^-$ $E1$ transitions connect the predominantly single-proton state $\pi i_{13/2}\otimes 0^+$ with the J_{max} and $J_{max}-1$ members of the $\pi h_{9/2}\otimes 2^+$ multiplet, and thus their relatively large $B(E1)$ values are surprising. However, the $\frac{13}{2}^+$ state can contain admixtures (in addition to $\pi f_{7/2}\otimes 3^-$), and one possible particle-core coupling candidate would be $\pi i_{11/2}\otimes 2^+$. The excitation energy of the $\pi i_{11/2}$ state is quite high[17] at 7.6 MeV. Starting from this component, however, the decays would proceed as allowed non-spin flip $\pi i_{11/2} \rightarrow \pi h_{9/2}$ transitions.

V. CONCLUSION

The high spin yrast states observed in ^{197}Bi can be interpreted in terms of the weak coupling of a valence proton to the predominantly two-quasiparticle (neutron-hole) states in the ^{196}Pb core. The excitation energies of these states fit well into the systematics for the heavier odd-A bismuth isotopes, and can be well reproduced by the cluster-interaction calculations described in Sec. IV. Configurations involving the $\pi i_{13/2}$ orbital play an increasingly important role as the excitation energy of this orbital drops with increasing neutron deficiency. No collective structures were observed in the yrast cascade. While there is a trend towards enhanced $E2$ transition probabilities as the neutron number decreases, no large increase in the collectivity would be required to explain these results. Thus, even 12 neutrons away from the closed shell, the observed states can be understood in terms of the shell model and weak coupling. In a subsequent paper,[9] a further extension of these studies to ^{195}Bi will be reported. Preliminary accounts of these results have been presented,[18] and are superceded by the present work.

ACKNOWLEDGMENTS

This work was supported in part by the National Science Foundation. One of us (K.D.) received financial support from the Danish National Science Research Council.

*Present address: Department of Physics, University of Pennsylvania, Philadelphia, PA 19104.

†Present address: Institute of Physics, University of Aarhus, DK-8000 Aarhus C, Denmark.

‡Present address: Department of Physics, University of Jyväskylä, SF-40100 Jyväskylä, Finland.

§Present address: Chalk River Nuclear Laboratories, Chalk River, Ontario, Canada K0J 1P0.

[1] W. F. Piel, Jr., T. Chapuran, K. Dybdal, D. B. Fossan, T. Lönnroth, D. Horn, and E. K. Warburton, Phys. Rev. C 31, 2087 (1985).

[2] T. Lönnroth, Z. Phys. A 307, 175 (1982).

[3] T. Lönnroth, J. Blomqvist, I. Bergström, and B. Fant, Phys. Scr. 19, 233 (1979).

[4] R. Brock, C. Günther, H. Hübel, A. Kleinrahm, D. Mertin, P. Meyer, and R. Tischler, Nucl. Phys. A278, 45 (1977).

[5] H. Hübel, A. Kleinrahm, C. Günther, D. Mertin, and R. Tischler, Nucl. Phys. A294, 177 (1978).

[6]R. Broda, C. Günther, and B. V. Thirumala Rao, Nucl. Phys. **A389**, 366 (1982).

[7]I. Bergström, C. J. Herrlander, P. Thieberger, and J. Blomqvist, Phys. Rev. **181**, 1642 (1969).

[8]M. Pautrat, G. Albouy, J. C. David, J. M. Lagrange, N. Poffé, C. Roulet, H. Sergolle, J. Vanhorenbeeck, and H. Abou-Leila, Nucl. Phys. **A201**, 449 (1973); G. Albouy, G. Auger, J. M. Lagrange, M. Pautrat, H. Richel, C. Roulet, H. Sergolle, and J. Vanhorenbeeck, *ibid.* **A303**, 521 (1978).

[9]T. Lönnroth, D. B. Fossan, W. F. Piel, Jr., M. A. Quader, S. Vajda, T. Chapuran, and E. K. Warburton (unpublished).

[10]K. Dybdal, T. Chapuran, D. B. Fossan, W. F. Piel, Jr., D. Horn, and E. K. Warburton, Phys. Rev. C **28**, 1171 (1983).

[11]L. Peker, Yad. Fiz. **1**, 27 (1966) [Sov. J. Nucl. Phys. **4**, 20 (1967)].

[12]I. Hamamoto, Phys. Rep. **10C**, 63 (1974).

[13]T. Lönnroth, Ph.D. thesis, University of Jyväskylä, 1980 (unpublished).

[14]I. Bergstrom and B. Fant, Phys. Scr. **31**, 26 (1985).

[15]R. Lutter, O. Häusser, D. J. Donahue, R. L. Hershberger, F. Reiss, H. Bohn, T. Faestermann, F. v. Feilitzsch, and K. E. G. Löbner, Nucl. Phys. **A229**, 230 (1974).

[16]H. E. Mahnke, T. K. Alexander, H. R. Andrews, O. Häusser, P. Taras, D. Ward, E. Dafni, and G. D. Sprouse, Phys. Lett. **88B**, 48 (1979).

[17]J. Speth, E. Werner, and W. Wild, Phys. Rep. **33C**, 127 (1977).

[18]T. E. Chapuran, K. Dybdal, D. B. Fossan, W. F. Piel, Jr., D. Horn, and E. K. Warburton, Bull. Am. Phys. Soc. **26**, 621 (1981); Proceedings of the 4th Nordic Meeting on Nuclear Physics, Fuglso, Denmark, 1982, p. 34.